THE JOURNAL OF PHYSICAL CHEMISTRY C

Article

pubs.acs.org/JPCC

Multiscale Study of Hydrogen Adsorption, Diffusion, and Desorption on Li-Doped Phthalocyanine Covalent Organic Frameworks

Jing-Hua Guo,[†] Hong Zhang,*[,†] Zhi-Pan Liu,[‡] and Xin-Lu Cheng[†]

[†]College of Physical Science and Technology, Sichuan University, Chengdu 610065, China

[‡]Shanghai Key Laboratory of Molecular Catalysis and Innovative Materials, Department of Chemistry, Fudan University, Shanghai 200433, China

ABSTRACT: In this paper, we performed a multiscale study on the hydrogen storage capacity of Li-doped phthalocyanine covalent organic frameworks (Li-doped Pc-PBBA COF). We combine the first-principles studies of hydrogen adsorption and migration energies with the kinetic Monte Carlo simulations of hydrogen adsorption, diffusion, and desorption processes in Li-doped Pc-PBBA COF. The first-principles calculations revealed that the Li atoms can be doped on the surface of the channel of Pc-PBBA COF with a binding energy of 1.08 eV. Each Li cation can bind three H_2 molecules with an average adsorption energy of 0.11 eV. At most, 24 H_2 molecules can be adsorbed in one formula unit, corresponding to a maximum of gravimetric density of 5.3 wt % and volumetric uptake of 45.2 g/L. The diffusion barriers of H_2 between different Li-adsorption sites are in the range 0.027−0.053 eV. The KMC simulations have predicted that the optimum conditions of hydrogen storage for Li-doped Pc-PBBA COF are at T = 250 K and P = 100 bar, with a gravimetric density of 4.70 wt % and volumetric uptake of 40.23 g/L. At T = 300 K and P = 1 bar, the adsorbed H_2 molecules have fast desorption kinetics, and 97% hydrogen can be released from the adsorbed phase to the gas phase. A two-step modification method (the B-substitution is first) was also advanced to suppress the Li clustering behavior and further improve the binding energy of H_2 molecules to doped Li atoms.

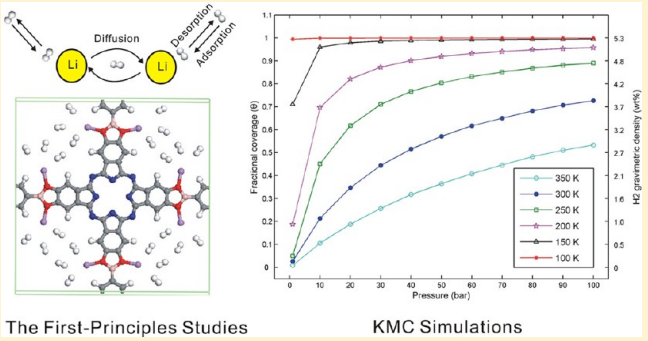

1. INTRODUCTION

Hydrogen storage is one of the main challenges in the realization of "The Hydrogen Economy". During the last two decades, many groups have been dedicated to developing a high-efficiency hydrogen storage method both in experiments and theory, including high pressure hydrogen storage tank,[1,2] liquid hydrogen,[1,3] metal hydrides,[4] complex hydrides,[5,6] porous solid materials,[7−10] and carbon-based nanostructures.[11−13] However, none has been shown experimentally to realize a hydrogen economy; a number of scientific and technical issues still remain. The storage of hydrogen has been identified as a central concern, especially in the on-board application to automobiles.

Since the covalent organic frameworks (COFs)[14] were first reported in 2005, they have attracted great attention due to the possibility for hydrogen storage. COFs are insoluble crystalline network solids containing micro- or mesopores exhibiting high surface areas ranging typically from 500 to 5600 m^2/g.[14−16] The highly ordered, uniform, porous architecture found in COFs is analogous to that observed for metal organic frameworks (MOFs).[17] Unlike MOFs, COF structures are entirely composed of light elements (H, B, C, and O); thus, they have extremely low densities (0.17 g/cm^3 for COF-108). H. Furukawa et al. have performed the isotherm measurements of hydrogen adsorbed in several COFs, and they showed that three-dimensional (3D) COFs can rival the best MOFs and other porous materials in their hydrogen uptake capacities (72.4 and 70.5 mg/g for COF-102 and COF-103, respectively, at 77 K).[10] S. S. Han et al. have carried out grand canonical Monte Carlo (GCMC) simulations for COFs, and they predicted that the maximum excess H_2 uptakes of COF-105 and COF-108 can reach 10 wt % under 77 K and 100 bar conditions.[18] On the basis of the molecular dynamics simulations, B. Assfour demonstrated that the COF structures are stable with hydrogen molecules adsorbed in it, and the adsorption interaction energy is found to be ∼0.03 eV.[19]

Recently, a new covalent organic framework, named Pc-PBBA COF, is synthesized by E. L. Spitler et al.[20] The Pc-PBBA COF features a square lattice composed of phthalocyanine macrocycles joined by phenylene bis(boronic acid) linkers (Figure 1). Pc-PBBA COF is a two-dimensional (2D) COF, which has a pore width of approximately 20 Å and an interlayer spacing of 3.34 Å. The evaluated Langmuir surface area and pore volume of Pc-PBBA COF are 506 m^2/g and 0.258 cm^3/g, respectively. The porous structure of Pc-PBBA COF provides

Received: April 22, 2012
Revised: July 11, 2012
Published: July 24, 2012

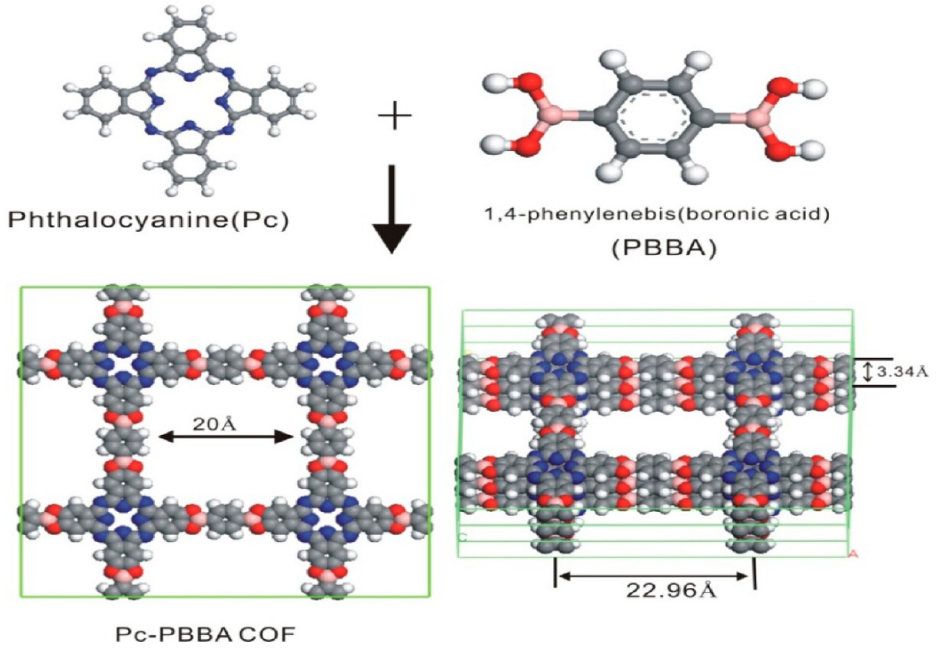

Figure 1. The Lewis-acid-catalyzed deprotection−condensation protocol was used to form the Pc-PBBA COF from phthalocyanine (Pc) tetra(acetonide) and PBBA. The pink, gray, white, red, and blue balls are boron, carbon, hydrogen, oxygen, and nitrogen atoms, respectively.

residence for hydrogen, which shows significant potential for hydrogen storage.

However, since the interactions of hydrogen with COFs are dominated by the van der Waals (vdW) and dispersion interactions, the COFs holding H_2 molecules require low operation temperatures and/or high pressures to guarantee a significant storage capacity. Neither the thermodynamics nor the storage capacity meets the requirements established for onboard applications.

In order to maximize the hydrogen adsorption uptake, the stable adsorption sites should be constructed in COFs. Earlier studies have shown that a positively charged metal atom (including transition metals and alkali metals, etc.) can bind a large amount of hydrogen in quasi-molecuar form due to the charge polarization mechanism, with a binding energy of 4.6−11.5 kcal/mol.[21,22] On the basis of this concept, a good method was advanced: decorating COFs with metal atoms. When metal atoms are deposited on COFs, charge transfer makes the metal atoms positively charged which then bind hydrogen quasimolecularly. The effects of metal-doping in COFs on hydrogen adsorption have been performed by several groups.[23−27] D.-P. Cao et al. have studied the Li-doping 3D COFs (COF-102, COF-103, COF-105, COF-108, and COF-202) on hydrogen storage performances by performing GCMC simulations, and they reported that the hydrogen uptakes of Li-doped COF-105 and COF-108 reach 6.84 and 6.73 wt % at T = 298 K and p = 100 bar, respectively, which are significantly higher than the capacities of pure COF-105 and COF-108.[23,24] Y. Y. Sun et al. explored ab initio calculations of hydrogen storage for Ca-decorated COF-α, and showed that Ca-decorated COF-α can store molecular hydrogen in both high gravimetric (5.7 wt %) and high volumetric (45 g L^{-1}) capacities.[25]

In this work, we focused on studying the effect of Li doping in Pc-PBBA COF on hydrogen adsorption to search for high capacity COF-based hydrogen storage materials. To validate the feasibility of the Li-doping measure, we need to address the following three issues. First, what sites do Li atoms like to occupy, and do they prefer to cluster? Does the metal doping affect the structure property of Pc-PBBA COF? Second, do the doped Li atoms bind a large amount of hydrogen with an ideal binding energy? Third, do hydrogen molecules uptake and release at a reasonable temperature? In view of the above issues, we carry out a detailed study of hydrogen adsorption, diffusion, and desorption using a multiscale simulation method. At first, the first-principles calculations were performed to study Li doping sites in Pc-PBBA COF. Following, we studied the impact of Li doping on hydrogen capture and hydrogen diffusion properties in Li-doped Pc-PBBA COF. Then, we performed kinetic Monte Carlo (KMC) simulation for hydrogen adsorption, diffusion, and desorption processes under different conditions. At last, we estimated the clustering behavior of Li atoms in Pc-PBBA COF and advanced a method to suppress it.

The KMC simulations will be of the greatest utility when they are linked in a hierarchy with the first-principles calculations, which can accurately describe the elementary steps and predict elementary energetic parameters.[28−31] F. Hess et al. have proved that the KMC simulations based on the first-principle parameters reproduce the experiment quite well.[31] By combining KMC simulations with first-principles calculations, we can study the evolution of kinetic behaviors of hydrogen with time in hydrogen storage medium. This enables us to explore the optimum conditions for hydrogen storage and release.

2. COMPUTATIONAL DETAILS

2.1. The First-Principles Calculations. The distribution scheme of Li in Pc-PBBA COF is determined using density functional theory and a plane-wave basis set with the projector augmented plane wave (PAW) method[32] as implemented in the Vienna ab initio simulation package (VASP).[33] The PW91 form was used for the generalized gradient approximation to exchange and correlation potential.[34] Previous benchmark calculations showed that the results using the PW91 functional

dx.doi.org/10.1021/jp305949q | J. Phys. Chem. C 2012, 116, 15908−15917

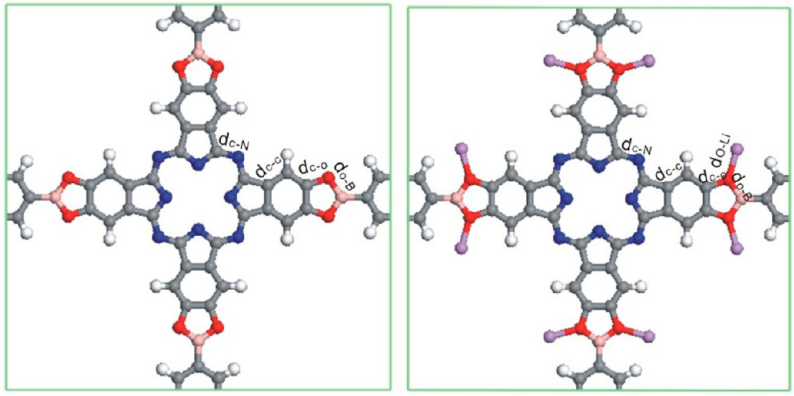

Figure 2. (a) The actual simulation cell in the first-principles calculations. (b) The Li atoms covalently attached to O atoms of the PBBA linker. The pink, gray, white, red, blue, and purple balls are boron, carbon, hydrogen, oxygen, nitrogen, and lithium atoms, respectively.

are close to those obtained from the MP2 level of theory for describing the noncovalent intermolecular interactions.[35−37] The valence states for all potentials used here are 1s for H, 2s2p for B, C, N, and O, and 1s2s for Li. The energy cutoff for the plane-wave basis set was 700 eV. The convergence for the energy and the force were set to 10^{-4} eV and 0.03 eV/Å, respectively. The periodic boundary condition is taken in all calculations, and the *k*-point is set to 1 × 1 × 2. The actual simulation cell in the first-principles calculations is presented in Figure 2a. A larger simulation cell and more *k*-points were also tested, which showed no significant difference in results. The climbing image nudged elastic band (CI-NEB) method was used to calculate the diffusion barrier for hydrogen diffusion between different adsorption sites. Initial and final states were selected on the basis of the adsorption calculations, and six images were chosen to derive smooth potential energy curves.

The average binding energy (B.E.) between the doped Li and COF is defined as

$$\text{B.E.} = [E(m\text{Li-COF}) - E(\text{COF}) - mE(\text{Li})]/m \quad (1)$$

where $E(m\text{Li-COF})$, $E(\text{COF})$, and $E(\text{Li})$ are the total energies of Pc-PBBA COF containing the doped Li atoms, of pure Pc-PBBA COF, and of a single Li atom, respectively. m is the number of Li atoms.

The energy gains ΔE_n by successive additions of H_2 molecules to Li-doped Pc-PBBA COF were calculated using the following formula:

$$\Delta E_n = E[\text{Li-COF}(H_2)_n] - E[\text{Li-COF}(H_2)_{n-1}] - E[H_2] \quad (2)$$

where $E[\text{Li-COF}(H_2)_n]$, $E(\text{Li-COF}(H_2)_{n-1})$, and $E(H_2)$ are the total energies of Pc-PBBA COF containing the adsorbed Li-nH_2 clusters, of Pc-PBBA COF containing the adsorbed Li atoms, and of H_2 in the gas phase, respectively. n is the number of H_2 molecules.

The average binding energy per H_2 molecule is computed by

$$\overline{\Delta E} = n_{\max}^{-1} \sum_{i=1}^{n_{\max}} \Delta E_i \quad (3)$$

2.2. Concept of the Kinetic Monte Carlo Scheme. The KMC simulation is one of the practical methods for studying the exact dynamical evolution of a system from state to state.[28,38] This approach has been applied in many fields, such as surface growth,[39,40] radiation damage,[41] adsorption/desorption phenomena,[42−44] et al. In our work, we used the Bortz−Kalos−Lebowitz (BKL) KMC algorithm, which has been quite successful in simulating kinetic behavior in Ising-like models.[45] The algorithm consists of the following steps:

(i) Count all the possible events at the current configuration and calculate the rates $r(i)$ (i = 1, 2, 3, ..., n, where n is the total number of events) of each event. Denote the total rates by $R = \sum_{i=1}^{n} r(i)$.

(ii) Generate a random number $\text{rand}_1 \in [0,1)$ and locate the kth event that satisfies the condition

$$\sum_{i=1}^{k} r(i) > R \times \text{rand}_1 > \sum_{i=1}^{k-1} r(i) \quad (4)$$

(iii) Generate the new configuration based on the chosen event k, and update the list of possible events. Assign a "real time" increment $\Delta t = -(1/R)\ln(\text{rand}_2)$ to this MC step, where rand_2 is another random number on [0, 1).

In the KMC simulations, a Langmuir type system is adopted, which means that we have a lattice of equal sites that can be occupied by only one molecule at a time and there are no further molecule−molecule interactions. The adsorption equilibrium (steady state) is established when the net rate of adsorption of H_2 in the gas phase is equal to the net rate of desorption of H_2 in the adsorbed phase. The appropriate kinetic expression for this balance is

$$\frac{d\theta}{dt} = r_A(1 - \theta) - r_D\theta = 0 \quad (5)$$

where θ is the fractional coverage of H_2, r_A is the rate of adsorption, and r_D is the rate of desorption.[28]

Using the kinetic gas theory, the rate of adsorption r_A can be calculated by converting the incoming flux of H_2 molecules into ML/s under the assumption of one monolayer to be 4.554 × $10^{18}/m^2$ adsorption sites (on the assumption that 24 H_2 molecules can be adsorbed in one unit cell of Li-doped Pc-PBBA COF).[46]

$$r_A = \frac{(pN_A)}{\sqrt{2\pi M_{H_2} RT}} \frac{1}{4.55 \times 10^{18}} = 4.1 \times 10^5 \frac{p}{\sqrt{T}} \quad (6)$$

where p is the pressure given in degrees Pa, N_A is Avogadro's constant, M_{H_2} is the molar mass of hydrogen, R is the gas

constant, and T is the simulation temperature given in degrees K.

The rate of diffusion $r(i)$ $(i = 2-6)$ and desorption r_D can be calculated on the basis of transition state theory and statistical mechanics, as given by[47]

$$r(i) = \nu \exp(-E_i/K_BT) = \frac{K_BT}{h} \exp(-E_i/K_BT) \quad (7)$$

$$r_D = \nu \exp(-E_D/K_BT) = \frac{K_BT}{h} \exp(-E_D/K_BT) \quad (8)$$

where K_B is the Boltzmann constant, h is Planck's constant, ν is the pre-exponential factor, which is chosen as $\nu = K_BT/h$, and E_i is the reaction barrier, which has been obtained in the first-principle calculation. Five diffusion pathways displayed in Figure 4a are considered in KMC simulation, and the diffusion barriers E_i $(i = 2, 6)$ are shown in section 3.3. The desorption energy E_D is equal to the average binding energy of an H_2 molecule bound to a doped Li atom. In our simulations, we ignore the binding energy between H_2 molecules, as the binding energy between molecules is very small.[48]

A three-dimensional lattice model is used to represent the adsorption sites of Li decorated Pc-PBBA COF. The size of the lattice is $2 \times 40 \times 40$, and periodic boundary conditions are employed. 1×10^{11} steps were performed for each run, with the first 1×10^8 steps taken to equilibrate the system and the following steps taken to sample the data every 1×10^8 steps. About 10^3 configurations were stored at each run, and the statistical results were obtained by averaging the output of 10^3 configurations.

3. RESULTS AND DISCUSSION

3.1. Doping of Li in Pc-PBBA COF. Generally, the metal atoms would be placed on top of the organic building blocks. This strategy has been successfully used in metal-doping for 3D COFs.[23,24] For Pc-PBBA COF, they have a narrow interlayer spacing (3.34 Å) but have a large channel (20 Å). If metal atoms are placed on the top of organic building blocks, they will locate between the two layers; thus, there will not be enough spacing for hydrogen adsorption. In our work, we attempt to introduce Li atoms on the side of building blocks. In this case, the doped Li atoms would appear on the surface of the channels.

We have carried out unconstrained geometry optimizations for Li-doped Pc-PBBA COF. As seen in Figure 2b, the Li atom covalently attached to the O atom of the PBBA linker with an average binding energy of 1.08 eV, and eight Li atoms can be introduced into one unit cell. The binding energies for Li doped on several COFs reported by previous studies[23,24,26] are summarized in Table 2. The binding energies of Li doped on different COFs are almost the same with each other, which are in the range 1.0−1.1 eV. The lattice parameters and some bond lengths of pure and Li-doped Pc-PBBA COF are presented in Table 1. The geometrical characteristics of Pc-PBBA COF obtained from our theoretical work are consistent with the experimental values.[20] As can be seen, Li induces a stretching of the C_2O_2B ring with an elongating of the C−O and B−O bonds, indicating that a charge transfer takes place from Li atoms to the COF framework. In fact, Bader analysis[49] of the self-consistent charge density revealed that the Li atoms carry a charge of +0.48e/Li, which is beneficial in raising the H_2 binding affinity. The previous studies (see Table 2) also showed that the doped Li atoms on COFs are positively charged with 0.3−0.54 e per Li atom.[23,24]

Table 1. The Lattice Parameters (Å) and Bond Lengths (Å) of Pure and Li-Doped Pc-PBBA COF[a]

material	$a = b$	c	d_{C-N}	d_{C-C}	d_{C-O}	d_{O-B}	d_{O-Li}
Pc-PBBA COF[b]	23.14	3.46	1.34	1.39	1.38	1.40	
Pc-PBBA COF[c]	22.96	3.34	1.46	1.39	1.36	1.45	
Li-doped COF[b]	23.22	3.56	1.34	1.40	1.43	1.42	1.92

[a]The lattice constants are denoted as a, b, and c. The C−N bond, C−C bond, C−O bond, O−B bond, and O−Li bond are marked in Figure 2. [b]The theoretical value in our work. [c]The experimental value from reference E. L. Spitler et al.[20]

Table 2. The Binding Energy per Li (B.E.) Atom on COFs, the Charge (q) Possessed by the Doped Li Atom, the Adsorption Energy per H_2 (ΔE), and the Hydrogen Uptake for Different Li-Doped COFs

	Li-COF10 ref 26	Li-3D COF[c] ref 23	Li-Pc PBBA COF	Li-COF202 ref 24
B.E. (eV/Li)	1.05	1.08	1.08	1.03
q (e)		0.3−0.5	0.48	0.31−0.54
ΔE (eV/H2)	0.11−0.15	0.10	0.11	0.10
H_2 uptake (wt %)		6.84[a]	5.30[b]	4.39[a]

[a]Predicted by GCMC simulation at 298 K and 100 bar. [b]Predicted by the first-principle calculation at 0 K. [c]Here, the 3D COF including COF-102, COF-103, COF-105, and COF-108.

We anticipate that the Li atoms can be impregnated into Pc-PBBA COF using lithium naphthalenide, which has been used to synthesize the Li-doped $Cu_3(BTC)_2$ and MIL-101(Cr).[50] In this method, the lithium naphthalenide is first prepared and then mixed with the Pc-PBBA COF. After several hours of stirring, the mixture is isolated by filtration and rinsing with tetrahydrofuran (THF) and then immersed in THF for 1 day to remove any weakly adsorbed naphthalene.

3.2. Adsorption of Hydrogen in Li-Doped Pc-PBBA COF. To investigate the hydrogen uptake, we optimized the structures with H_2 molecules placed in the vicinity of the Li atoms. In Figure 3a, we display the optimized geometries as the H_2 uptake increases from one to three molecules around the Li atom. Actually, no more than three hydrogen molecules could be adsorbed around each Li atom. The adsorption energies calculated by eq 1 are 0.094 eV for the first H_2 molecule, 0.118 eV for the second H_2 molecule, and 0.117 eV for the third H_2 molecule. The average binding energy calculated by eq 2 is 0.11 eV. Our calculation results are consistent with the previously reported 0.10−0.15 eV for the interaction of H_2 with a Li cation doped in COFs,[23,24,26] which can be seen in Table 2. The H−H bond length is elongated to 0.76 Å due to the charge polarization mechanism, compared with the H−H bond distance in the free molecule which is 0.75 Å.

Because each formula unit can contain eight Li atoms, 24 H_2 molecules can be adsorbed (Figure 3b), corresponding to a maximum of gravimetric density of 5.3 wt % and volumetric uptake of 45.2 g/L. Figure 3c shows the optimized structures of hydrogen adsorption in pure Pc-PBBA COF. Sixteen H_2 molecules can be adsorbed in each formula unit, corresponding to a gravimetric density of 3.7 wt % and volumetric uptake of 27.7 g/L. Compared to the H_2 adsorption in pure Pc-PBBA

dx.doi.org/10.1021/jp305949q | J. Phys. Chem. C 2012, 116, 15908−15917

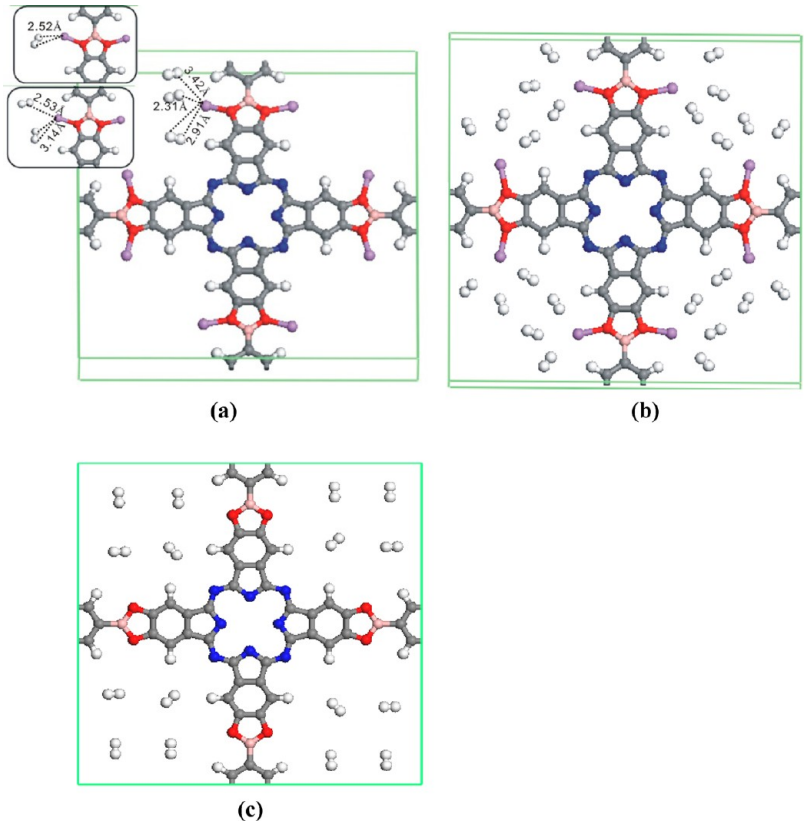

Figure 3. Optimized structures of hydrogen adsorption in pure and Li-doped Pc-PBBA COF. (a) Sequential H_2 adsorption (up to three H_2) on a Li atom. (b) Li-doped Pc-PBBA COF with fully loaded H_2. (c) Pure Pc-PBBA COF with fully loaded H_2.

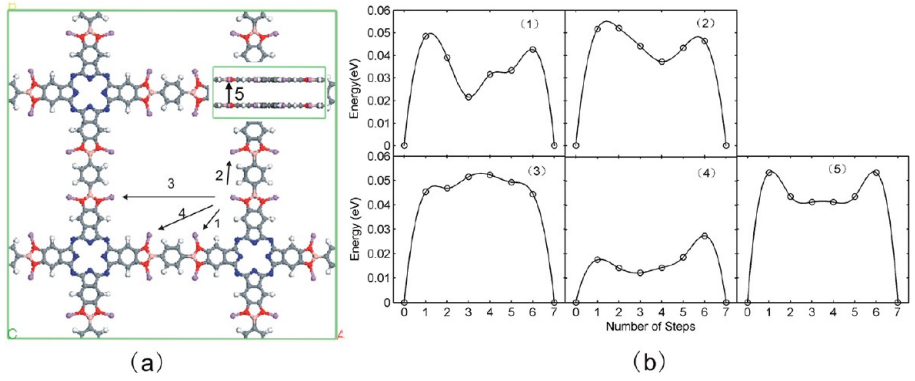

Figure 4. (a) Illustration of the diffusion pathways which have been considered in this work. (b) The calculated migration barriers corresponding to the migration routes displayed in part a. The line is drawn as a guide to the eye.

COF that the H_2 molecules equably distributed on the 1D-channel of pure Pc-PBBACOF, the H_2 molecules are bound around the Li sites in Li-doped Pc-PBBA COF. Thus, we can say that the direct reason for the improved H_2 uptake of Pc-PBBA COF is the strong interaction between lithium and hydrogen.

3.3. The Diffusion of Hydrogen in Li-Doped Pc-PBBA COF. In this section, we investigate the diffusion behavior of H_2 molecule in Li decorated Pc-PBBA COF by CI-NEB calculations. Five diffusion pathways are considered in this work, as shown in Figure 4a. Figure 4b shows the calculated minimum energy path for a single H_2 molecule migrating from one adsorption site to another adjacent adsorption site. We ignore the intermolecular interaction between H_2 molecules, as the interaction between them is very small. The diffusion barriers for the five routes are 0.048, 0.053, 0.052, 0.027, and 0.053 eV, respectively, which is 0.2−0.5 times of the adsorption energy. The results obtained from density functional theory (DFT) calculations are used as input to kinetic Monte Carlo simulations. Considering the small diffusion barriers, it is likely that the H_2 migration behaviors may coexist at low temperatures. Clearly, the diffusion barrier of route 4 is lower than that of other routes, due to this route across the scope of an adjacent Li atom. From Figure 4b, the intermediate adsorption sites, originated from the potential fields of Pc-PBBA COF skeleton atoms, can be found at routes 1 and 2. Their positions at the vicinity of Pc macrocycles and the side of benzene ring, with adsorption energy of 0.064 and 0.059 eV, respectively.

3.4. KMC Simulation for H_2 Adsorption, Diffusion, and Desorption. The exploration of the optimum conditions for

dx.doi.org/10.1021/jp305949q | J. Phys. Chem. C 2012, 116, 15908−15917

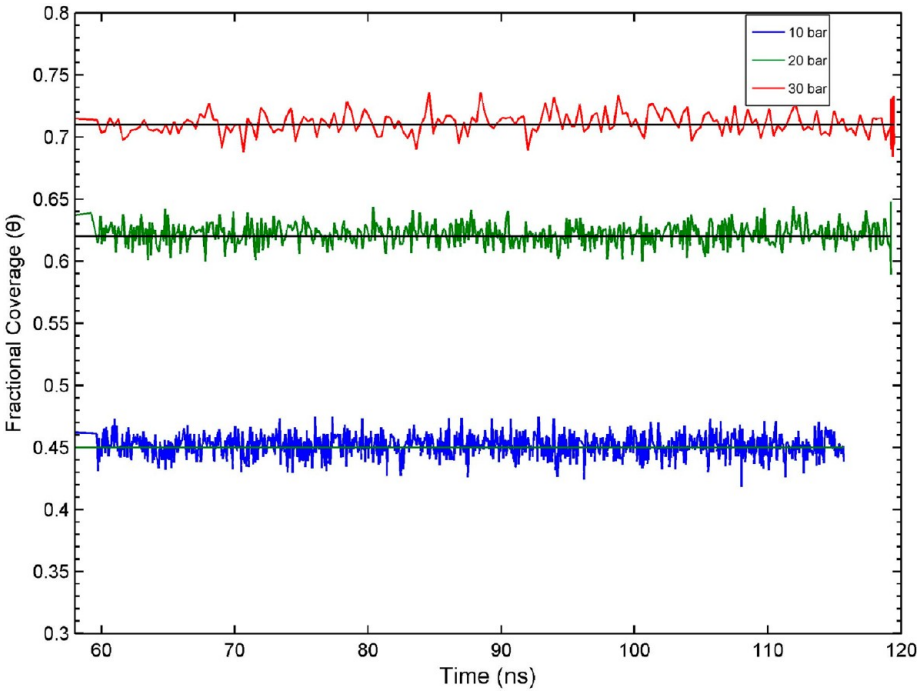

Figure 5. The transient fractional coverage (θ) of hydrogen after 60 ns (10^8 steps) evolution at T = 250 K and P = 10, 20, and 30 bar, respectively. The black lines denoted the exact solution of eq 5.

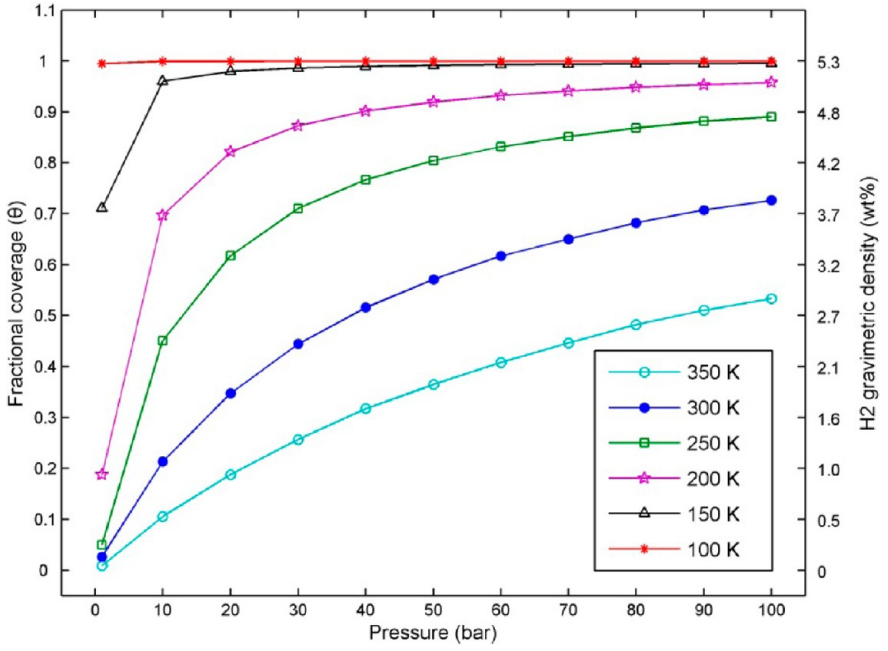

Figure 6. The fractional coverage (θ) of hydrogen after the adsorption equilibriums established in different environments (T = 100−350 K, P = 1−100 bar).

hydrogen storage and release is very important in designing hydrogen storage materials. GCMC simulation is a commonly used technique to study the adsorption properties of H_2 under different conditions. However, the evolution of kinetic behaviors of hydrogen with time cannot be studied in GCMC simulation. Here we perform KMC simulations for the kinetic behaviors of hydrogen molecule in Li-doped Pc-PBBA COF under different conditions. The dynamics of the system is described as stochastic processes including adsorption, diffusion, and desorption.

Figure 5 depicts the transient fractional coverage (θ) of hydrogen after 60 ns (10^8 steps) evolution at T = 250 K and P = 10, 20, and 30 bar, respectively. The black lines denoted the exact solution of eq 5, which reflected the detailed balance of the adsorption−desorption model. It can see that the adsorption equilibriums have been established after 10^8 steps. There is excellent agreement between the transient solution of Monte Carlo simulation and the exact solution of eq 5. Our KMC program is executable for simulating the adsorption−desorption model.

dx.doi.org/10.1021/jp305949q | J. Phys. Chem. C 2012, 116, 15908−15917

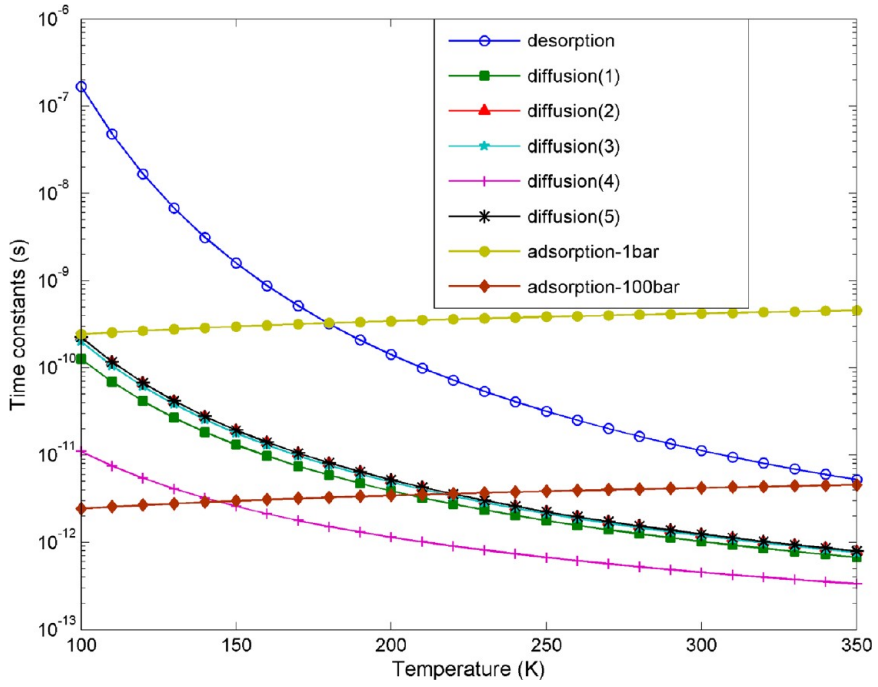

Figure 7. The time constants of adsorption, desorption, and diffusion behaviors along five pathways plotted as a function of temperature from 100 to 300 K.

To investigate the optimum conditions for hydrogen storage and release in Li-doped Pc-PBBA COF, we performed KMC simulations at T = 100, 150, 200, 250, and 300 K in the pressure range from 1 to 100 bar. Figure 6 depicts the fractional coverage (θ) of hydrogen after the adsorption equilibriums established in different environments. At room temperature (300 K), the maximum coverage is 0.72 at P = 100 bar, corresponding to a gravimetric density of 3.81 wt % and a volumetric uptake of 32.50 g/L, which is below the saturation level (5.30 wt % and 45.20 g/L) found from 0 K calculations. This result is due to the dynamical effects that the adsorption behaviors and desorption behaviors of H_2 occurred simultaneously in the real adsorption procedure. A similar finding has been reported that the ab initio molecular dynamics calculation shows a hydrogen uptake of 2.0 wt % at 300 K, which is below the saturation level (4.3 wt %) predicted by DFT calculation.[51] When the temperature is lower than 150 K, due to the minor rate of desorption, which is 10^{-2}–10^{-5} times the rate of adsorption, the coverage of hydrogen nearly reaches saturation level. The USA Department of Energy (DOE) has set the 2010 targets of 4.5 wt % and 28 g/L and the 2017 targets of 5.5 wt % and 40 g/L.[52,53] As seen from Figure 6, the maximum temperature at which the 2010 targets can be realized is T = 250 K. At T = 250 K and p = 100 bar, the gravimetric density reached 4.70 wt % and the volumetric uptake reached 40.23 g/L. Though the hydrogen storage capacity of Li-doped Pc-PBBA COF cannot reach the 2017 target on a gravimetric basis, the 2017 target on a volumetric basis can be realized at T = 200 K and P = 40 bar. DOE has propounded that the operating ambient temperature of onboard hydrogen storage is 233–333 K (−40–60 °C), and the max delivery pressure is 100 bar.[53] Thus, the optimum conditions of hydrogen storage are T = 250 K and P = 100 bar for Li-doped Pc-PBBA COF.

Due to the rate of desorption increase with increasing temperature, the thermodynamic driving force for hydrogen desorption is increased. At T = 300 K and P = 1 bar, the rate of desorption is about 10^2 times the rate of adsorption; thus, the coverage of hydrogen reduced to 0.03, which means that 97% hydrogen can be released from the adsorbed phase to the gas phase. We can say that the Li-doped COF is an efficient onboard storage system that greater than 90% hydrogen can be released at room temperature. Our simulation results also indicated that the binding energy of 0.11 eV is suitable for hydrogen delivery, which is consistent with the previous study that an adsorption energy of 0.15 eV is desired for optimum delivery of hydrogen at T = 298 K.[54]

The time-scale of a kinetic behavior can be represented by its time constant (τ), which can be converted by inverting the rate constant determined from eqs 5–7. In Figure 7, the time constants of adsorption, desorption, and diffusion behaviors along five pathways are plotted as a function of temperature from 100 to 350 K. From the figure, we can see that the time constant of adsorption has a slow change in the range of 10^{-10}–10^{-9} s for P = 1 bar and 10^{-12}–10^{-11} s for P = 100 bar, due to it being proportional to $T^{1/2}$. The time constants of desorption, namely, residence time, have a large change from 10^{-7} s at the low temperature region to 10^{-11} s at the high temperature region. Due to a longer residence time at low temperature, the coverage of hydrogen nearly reached saturation level. At a high pressure (P = 100 bar), the residence time is larger than the time constant of adsorption at the whole temperature range, which indicated that the H_2 molecule can be stored in Li-doped Pc-PBBA COF at the environment of high pressure. At room temperature and low pressure (P = 1 bar), the short residence time indicates that the adsorbed H_2 molecules have fast desorption kinetics, which assured that the hydrogen can be released in a short time. Notice that the time constants of diffusion are small in comparison to the residence time, indicating the great relative fluidity of H_2 molecules in Li-doped Pc-PBBA COF.

3.5. The Clustering Behavior of Li Atoms in Pc-PBBA COF and How to Suppress It. As shown in Table 2, the

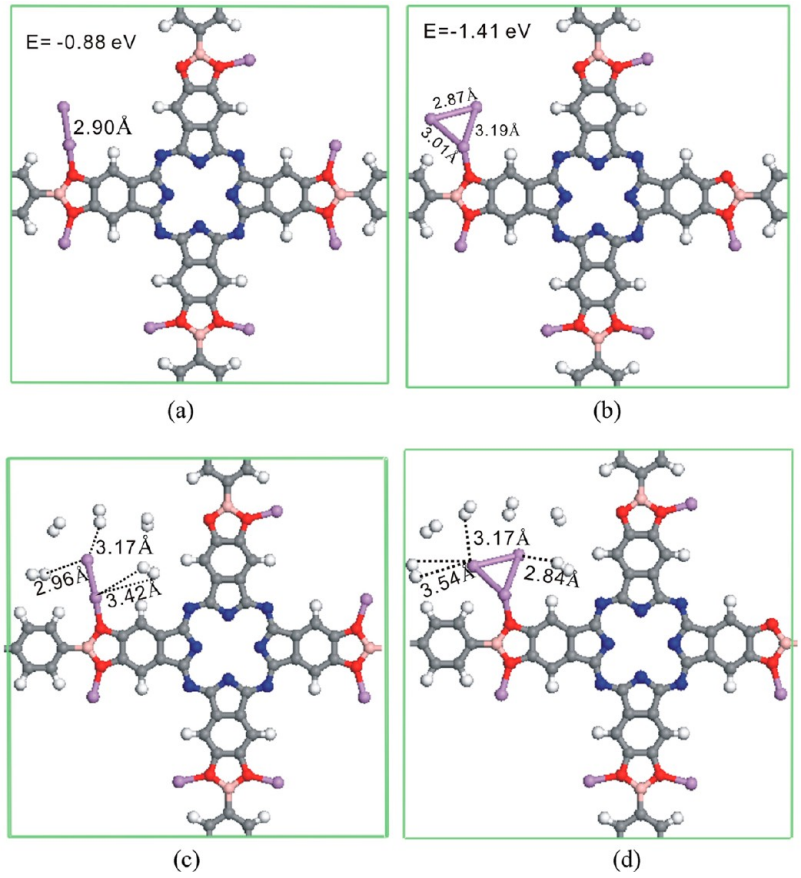

Figure 8. Optimized geometry for Li dimer (a) and trimer (b) in Pc-PBBA COF. The relative energy E is evaluated referring to the isolated configuration shown in Figure 2b. (c) H_2 adsorption on Li dimer. (d) H_2 adsorption on Li trimer.

binding energies of Li doped on COFs are in the range of 1.0−1.1 eV, which is lower than the cohesive energy of bulk Li (1.63 eV).[55] Thus, they tend to form clusters on the surface of COFs. We study here the aggregation of Li atoms in Pc-PBBA COF. When a Li atom is put on the position at 3.0 Å near another Li atom bound on Pc-PBBA COF, the Li atoms are aggregated (Figure 8a), which is energetically more favorable by 0.88 eV than separated Li atoms. As shown in Figure 8b, the Li trimer can be formed when the third Li atom approaches the Li dimer, with the energy of 1.41 eV lower than the separated Li atoms. Due to the steric hindrance between H_2 molecules, at most five and six H_2 molecules can be attached to the Li dimer and Li trimer (Figure 8c,d), with an average adsorption energy of 0.13 and 0.12 eV, respectively. For isolated Li atoms in Pc-PBBA COF, each can adsorb three H_2 molecules. Thus, we see that the aggregation of Li atoms reduces the storage capacity.

In order to achieve a successful hydrogen storage using Li decoration, clustering of Li metal atoms should be suppressed. As a way to overcome such clustering, it was suggested to increase the binding strength between metal and COFs by chemical modification, such as C atoms in COFs can be partially substituted by B atoms.[56] Here we attempted the chemical doping of the bridge C_2O_2B ring in Pc-PBBA COF by replacing the C elements with B elements. The optimized geometry is presented in Figure 9a. In the experiment, it has realized to substitute the C atoms by B atoms in carbon-based systems.[57,58] B substitution for C introduces hole carriers into COFs, and the prominent acceptor state is present in the B-doped COFs, which facilitates the charge transfer from the adsorbed metal atoms to COFs.[56]

We next introduced the Li atoms to the B-substitution Pc-PBBA COF. After optimization, the Li atom attached to O and B atoms of PBBA linker, as shown in Figure 9b, with an average binding energy of 2.06 eV. Clearly, the B substitution has increased the binding energy of Li atoms to Pc-PBBA COF, which is larger than the Li bulk cohesive energy (1.63 eV). Thus, the clustering of Li atoms would be suppressed. In fact, in B-substitution Pc-PBBA COF, the isolated Li_8 configuration (Figure 9b) is 1.01 eV lower in energy than the clustered configuration (two Li atoms formed Li dimer, as seen in Figure 9c). Bader charge analysis revealed that the Li atoms carry a charge of +0.85e/Li, which is larger than that of Li atoms (+0.48e/Li) doped in pristine Pc-PBBA COF. The B-substitution actually increases the charge transfer from the Li atoms to Pc-PBBA COF; thus, the binding strength between Li atoms and Pc-PBBA COF is increased. Because the Li atoms in B-substitution Pc-PBBA COF carry a larger positive charge, this results in a higher binding energy of H_2. The average adsorption energy is 0.17 eV for three H_2 molecules successively adsorbed in one Li atom, which has been enhanced about 55% compared with that (0.11 eV) for Li doping in pristine Pc-PBBA COF.

4. CONCLUSIONS

In summary, a multiscale study that combines the first-principles calculations with kinetic Monte Carlo simulations has been performed to study the hydrogen storage capacity of

dx.doi.org/10.1021/jp305949q | J. Phys. Chem. C 2012, 116, 15908−15917

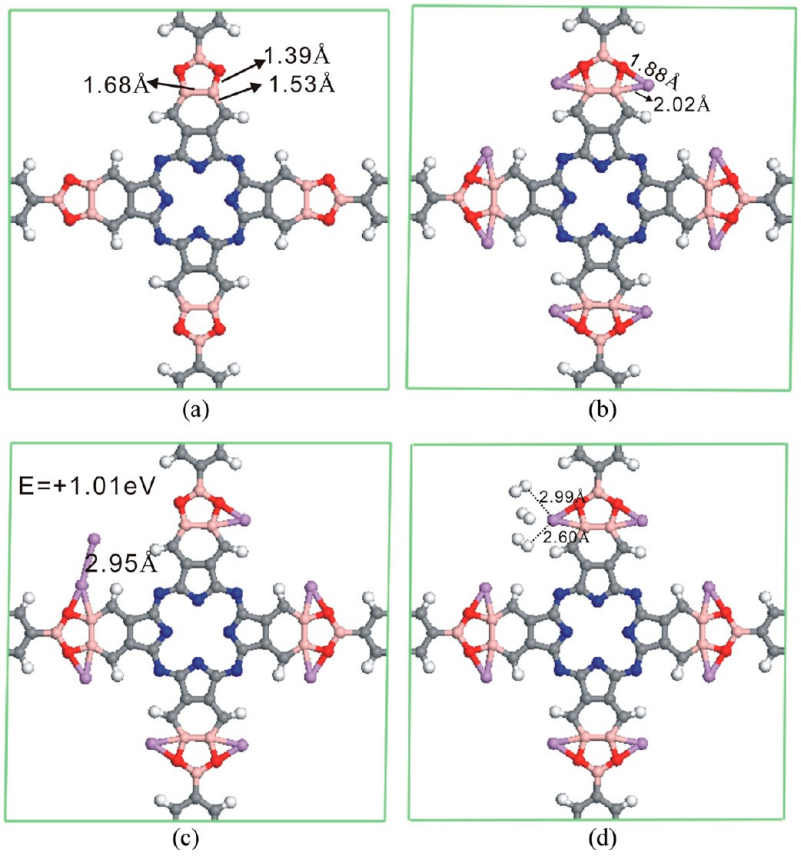

Figure 9. Optimized geometry for (a) B-substitution Pc-PBBA COF, (b) Li-doped B-substitution Pc-PBBA COF, (c) Li dimer in B-substitution Pc-PBBA COF, and (d) three H_2 adsorbed on one Li atom. The relative energy E in part c is evaluated referring to the isolated configuration shown in part b.

Li-doped Pc-PBBA COF. The first-principles calculations revealed that the Li atom can be doped on the surface of the channel of Pc-PBBA COF with a binding energy of 1.08 eV. The doped Li atoms are positively charged, and each Li cation can bind three H_2 molecules with the average adsorption energy of 0.11 eV. In total, 24 H_2 molecules can be adsorbed in one formula unit, corresponding to a maximum of gravimetric density of 5.3 wt % and volumetric uptake of 45.2 g/L. The diffusion barriers of H_2 between different Li-adsorption sites are in the range of 0.027−0.053 eV, which is about 0.2−0.5 times the adsorption energy. The KMC simulations have predicted that the optimum conditions of hydrogen storage for Li-doped Pc-PBBA COF are at T = 250 K and P = 100 bar, with a gravimetric density 4.70 wt % and volumetric uptake 40.23 g/L. At T = 300 K and P = 1 bar, the adsorbed H_2 molecules have fast desorption kinetics, and 97% hydrogen can be released from the adsorbed phase to the gas phase. To suppress the clustering of Li atoms, we advanced a two-step modification method, in which the Pc-PBBA COF was first chemically modified with B doping, and then the Li atoms doped in B-substitution Pc-PBBA COF. The B modification not only suppressed the clustering of Li atoms but also improved the binding energy of H_2 to doped Li atoms.

In this work, we not only predicted a good hydrogen storage material, which reaches the 2010 target set by DOE, but we also have shown here a route to study the hydrogen adsorption, diffusion, and desorption, i.e., the combining of the first-principles calculations with KMC simulations.

AUTHOR INFORMATION

Corresponding Author

*E-mail: hongzhang@scu.edu.cn. Phone: +86-28-85400158.

Notes

The authors declare no competing financial interest.

ACKNOWLEDGMENTS

H.Z. acknowledges financial support from the National Natural Science Foundation of China (NSFC Grant No. 11074176 and NSAF Grant No. 10976019) and the support from Research Fund for the Doctoral Program of Higher Education of China (Grant No. 20100181110080)

REFERENCES

(1) Züttel, A. *Mater. Today* **2003**, *6*, 24.
(2) Cumalioglu, I.; Ma, Y.; Ertas, A.; Maxwell, T. *J. Pressure Vessel Technol.* **2007**, *129*, 216.
(3) Aceves, S. M.; Berry, G. D. *J. Energy Resour. Technol.* **1998**, *120*, 137.
(4) Tang, F.; Yuan, W.; Lu, T. M.; Wang, G. C. *J. Appl. Phys.* **2008**, *104*, 033534.
(5) Bogdanović, B.; Schwickardi, M. *J. Alloys Compd.* **1997**, *1*, 253.
(6) Huot, J.; Liang, G.; Schulz, R. *J. Alloys Compd.* **2003**, *353*, L12.
(7) Rosi, N. L.; Eckert, J.; Eddaoudi, M.; Vodak, D. T.; Kim, J.; O'Keeffe, M.; Yaghi, O. M. *Science* **2003**, *300*, 1127.
(8) Han, S. S.; Choi, S.-H.; Goddard, W. A., III. *J. Phys. Chem. C* **2010**, *114*, 12039.
(9) Li, A.; Lu, R.-F.; Wang, Y.; Wang, X.; Han, K.-L.; Deng, W.-Q. *Angew. Chem., Int. Ed.* **2010**, *49*, 3330.
(10) Furukawa, H.; Yaghi, O. M. *J. Am. Chem. Soc.* **2009**, *131*, 8875.

(11) Dillon, A. C.; Jones, K. M.; Bekkedahl, T. A.; Kiang, C. H.; Bethune, D. S.; Heben, M. J. *Nature* **1997**, *386*, 377.
(12) Kruse, H.; Grimme, S. *J. Phys. Chem. C* **2009**, *113*, 17006.
(13) Okamoto, Y.; Miyamoto, Y. *J. Phys. Chem. B* **2001**, *105*, 3470.
(14) Côté, A. P.; Benin, A. I.; Ockwig, N. W.; O'Keeffe, M.; Matzger, A. J.; Yaghi, O. M. *Science* **2005**, *310*, 1166.
(15) El-Kaderi, H. M.; Hunt, J. R.; Mendoza-Cortes, J. L.; Côté, A. P.; Taylor, R. E.; O'Keeffe, M.; Yaghi, O. M. *Science* **2007**, *316*, 268.
(16) Côté, A. P.; El-Kaderi, H. M.; Furukawa, H.; Hunt, J. R.; Yaghi, O. M. *J. Am. Chem. Soc.* **2007**, *129*, 12914.
(17) Chen, B.; Eddaoudi, M.; Hyde, S. T.; O'Keeffe, M.; Yaghi, O. M. *Science* **2001**, *291*, 1021.
(18) Han, S. S.; Furukawa, H.; Yaghi, O. M.; Goddard, W. A., III. *J. Am. Chem. Soc.* **2008**, *130*, 11580.
(19) Assfour, B.; Seifert, G. *Chem. Phys. Lett.* **2010**, *489*, 86.
(20) Spitler, E. L.; Dichtel, W. R. *Nat. Chem.* **2010**, *2*, 672.
(21) Niu, J.; Rao, B. K.; Jena, P. *Phys. Rev. Lett.* **1992**, *68*, 2277.
(22) Rao, B. K.; Jena, P. *Europhys. Lett.* **1992**, *20*, 307.
(23) Cao, D.; Lan, J.; Wang, W.; Smit, B. *Angew. Chem., Int. Ed.* **2009**, *48*, 4730.
(24) Lan, J.; Cao, D.; Wang, W. *J. Phys. Chem. C* **2010**, *114*, 3108.
(25) Sun, Y. Y.; Lee, K.; Kim, Y.-H.; Zhang, S. B. *Appl. Phys. Lett.* **2009**, *95*, 033109.
(26) Wu, M. M.; Wang, Q.; Sun, Q.; Jena, P.; Kawazoe, Y. *J. Chem. Phys.* **2010**, *133*, 154706.
(27) Choi, Y. J.; Lee, J. W.; Choi, J. H.; Kang, J. K. *Appl. Phys. Lett.* **2008**, *92*, 173102.
(28) Fichthorn, K. A.; Weinberg, W. H. *J. Chem. Phys.* **1991**, *95*, 1090.
(29) Hansen, E. W.; Neurock, M. *J. Catal.* **2000**, *196*, 241.
(30) Reuter, K.; Frenkel, D.; Scheffler, M. *Phys. Rev. Lett.* **2004**, *93*, 116105.
(31) Hess, F.; Farkas, A.; Seitsonen, A. P.; Over, H. *J. Comput. Chem.* **2012**, *33*, 757.
(32) Kresse, G.; Joubert, D. *Phys. Rev. B* **1999**, *59*, 1758.
(33) Kresse, G.; Furthmuller, J. *Comput. Mater. Sci.* **1996**, *6*, 15.
(34) Perdew, J. P.; Wang, Y. *Phys. Rev. B* **1992**, *45*, 13244.
(35) Tsuzuki, S.; Lüthi, H. P. *J. Chem. Phys.* **2011**, *114*, 3949.
(36) Sun, Y. Y.; Lee, K.; Wang, L.; Kim, Y.-H.; Chen, W.; Chen, Z.; Zhang, S. B. *Phys. Rev. B* **2010**, *82*, 073401.
(37) Wesolowski, T. A.; Parisel, O.; Ellinger, Y.; Weber, J. *J. Phys. Chem. A* **1997**, *101*, 7818.
(38) Voter, A. F. Introduction to the Kinetic Monte Carlo Method. In *Radiation Effects in Solids*; Sickafus, K. E., Kotomin, E. A., Eds.; Springer, NATO Publishing Unit: Dordrecht, The Netherlands, 2005.
(39) Nurminen, L.; Kuronen, A.; Kaski, K. *Phys. Rev. B* **2000**, *63*, 035407.
(40) Tan, X.; Ouyang, G.; Yang, G. W. *Phys. Rev. B* **2006**, *73*, 195322.
(41) Beeler, J. R., Jr. *Phys. Rev.* **1966**, *150*, 470.
(42) Abraham, F. F.; White, G. M. *J. Appl. Phys.* **1970**, *41*, 1841.
(43) Lehner, B.; Hohage, M.; Zeppenfeld, P. *Surf. Sci.* **2000**, *454*, 251.
(44) Petrova, N. V.; Yakovkin, I. N. *Eur. Phys. J. B* **2008**, *63*, 17.
(45) Bortz, A. B.; Kalos, M. H.; Lebowitz, J. L. *J. Comput. Phys.* **1975**, *17*, 10.
(46) Abild-Pedersen, F.; Lytken, O.; Engbæk, J.; Nielsen, G.; Chorkendorff, I.; Nørskov, J. K. *Surf. Sci.* **2005**, *590*, 127.
(47) Tang, Q.-L.; Hong, Q.-J.; Liu, Z.-P. *J. Catal.* **2009**, *263*, 114.
(48) Tan, X.; Yang, G. W. *J. Phys. Chem. C* **2008**, *112*, 4219.
(49) Henkelman, G.; Arnaldsson, A.; Jónsson, H. *Comput. Mater. Sci.* **2006**, *36*, 354.
(50) Xiang, Z.; Hu, Z.; Yang, W.; Cao, D. *Int. J. Hydrogen Energy* **2012**, *37*, 946.
(51) Blomqvist, A.; Araújo, C. M.; Srepusharawoot, P.; Ahuja, R. *Proc. Natl. Acad. Sci. U.S.A.* **2007**, *104*, 20173.
(52) USDOE *Office of Energy Efficiency and Renewable Energy, The FreedomCAR and Fuel Partnership, Targets for Onboard Hydrogen Storage Systems for Light-Duty Vehicles,* https://www1.eere.energy.gov/hydrogenandfuelcells/storage/pdfs/targets_onboard_hydro_storage_explanation.pdf, 2009.
(53) USDOE; USCAR; Shell; BP; ConocoPhillips; Chevron; ExxonMobil *The FreedomCAR and Fuel Partnership, Multi-Year Research, Development and Demonstration Plan,* http://www1.eere.energy.gov/hydrogenandfuelcells/mypp/pdfs/storage.pdf, 2009.
(54) Bhatia, S. K.; Myers, A. L. *Langmuir* **2006**, *22*, 1688.
(55) Sun, Q.; Jena, P.; Wang, Q.; Marquez, M. *J. Am. Chem. Soc.* **2006**, *128*, 9741.
(56) Zou, X.-L.; Zhou, G.; Duan, W.-H.; Choi, K.; Ihm, J. *J. Phys. Chem. C* **2010**, *114*, 13402.
(57) Way, B. M.; Dahn, J. R.; Tiedje, T.; Myrtle, K.; Kasrai, M. *Phys. Rev. B* **1992**, *46*, 1697.
(58) Shirasaki, T.; Derre, A.; Menetrier, M.; Tressaud, A.; Flandrois, S. *Carbon* **2000**, *38*, 1461.